CSIRO PUBLISHING

www.publish.csiro.au/journals/ijwf *International Journal of Wildland Fire* **2008**, *17*, 131–146

Long-term impacts of prescribed burns on soil thermal conductivity and soil heating at a Colorado Rocky Mountain site: a data/model fusion study

W. J. Massman[A,C], *J. M. Frank*[A] *and N. B. Reisch*[B]

[A]USDA Forest Service, Rocky Mountain Research Station, 240 West Prospect, Fort Collins, CO 80526, USA.
[B]Anadarko Industries, 500 Dallas, Suite 2950, Houston, TX 77002, USA.
[C]Corresponding author. Email: wmassman@fs.fed.us

Abstract. Heating any soil during a sufficiently intense wild fire or prescribed burn can alter that soil irreversibly, resulting in many significant, and well studied, long-term biological, chemical, and hydrological effects. On the other hand, much less is known about how fire affects the thermal properties and the long-term thermal regime of soils. Such knowledge is important for understanding the nature of the soil's post-fire recovery because plant roots and soil microbes will have to adapt to any changes in the day-to-day thermal regime. This study, which was carried out at Manitou Experimental Forest (a semiarid site in the Rocky Mountains of central Colorado, USA), examines three aspects of how fire can affect the long-term (post-fire) thermal energy flow in soils. First, observational evidence is presented that prescribed burns can alter the thermal conductivity of soils to a depth of at least 0.2 m without altering its bulk density. Second, data are presented on the thermal properties of ash. (Such data are necessary for understanding and modeling the impact any remaining post-fire ash layer might have on the daily and seasonal flow of thermal energy through the soil.) Third, observational data are presented on the long-term effects that prescribed burns can have on soil surface temperatures. In an effort to quantify long-term changes in the soil temperatures and heat fluxes resulting from fire this study concludes by developing and using an analytical model of the daily and annual cycles of soil heating and cooling, which incorporates observed (linear variation of) vertical structure of the soil thermal properties and observed changes in the surface temperatures, to synthesise these fire-induced effects. Modeling results suggest that under the dry soil conditions, typical of the experimental forest, the amplitudes of the daily and seasonal cycles of soil heating/cooling in the fire-affected soils will greatly exceed those in the soils unaffected by fire for several months to years following the fire and that these effects propagate to depths exceeding one metre.

Additional keywords: fire, ponderosa pine, soil heat flux, soil microclimate.

Introduction

Fire's impact on soils can vary between highly beneficial, when the fire is not too intense and soil heating brief, to irreversible damage, which occurs during deeply penetrating heat pulses and longer-term exposures (DeBano *et al.* 1999, 2005). The primary factor determining the degree of impact is the type and amount of fuel available for burning. In the case of a prescribed slash pile burn often the fuel loading is relatively high (compared to what might occur naturally) and the length of time the soil is exposed to burning materials can last several hours or days (e.g. Massman and Frank 2004). Consequently, slash pile burning, although an effective management tool for reducing the risk of a catastrophic wildfire, has the potential to significantly impact (or alter the characteristics of) the soil underlying the pile itself. Because of the severity of the soil heating during a prescribed slash pile burn these impacts can be significant and serious. They include the formation of a hydrophobic layer on the surface of or within the soil, destruction of most of the organic material in the upper few centimeters of soil and the concomitant loss of soil aggregate stability, changes in soil pH and soil chemistry, long-term differences in soil moisture amounts, increases in soil bulk density with accompanying decreases in soil porosity, and changes to soil structure (DeBano *et al.* 1999; Huffman *et al.* 2001; Badía and Martí 2003; Seymour and Tecle 2004; Knoepp *et al.* 2005; Neary and Ffolliott 2005; Massman *et al.* 2006).

While these and other fire-induced effects have been studied and are reasonably well understood, changes in the soil's thermal regime that result from fire-associated soil heating and that persist with duration greater than a year have (to our knowledge) never been previously examined. But, knowledge of any fire-induced changes in the thermal regime of soils is integral to describing the environment that soil microbes and plant roots must adapt to if they are to recover from or survive a fire.

Of the many fire-induced changes to soils, the most relevant to the long-term thermal regime are changes in the soil surface associated with radiationally-driven soil heating and cooling and alterations in the soil structure that may facilitate changes to the thermal properties of the soil. [Note: (*a*) By changes in the thermal properties of soils we are not referring to short-term

 10.1071/WF06118 1049-8001/08/010131

changes caused by the reduction (vaporisation) of soil moisture during a fire. Rather we mean changes in the intrinsic or dry-soil values of these properties and changes to the sensitivity of these properties to soil moisture when the soil is moist. (*b*) By soil structure we mean the way in which soil particles and soil aggregates and their contact surfaces are organised within and define the soil matrix.]

Changing the albedo of the soil surface, such as fire-scarring (blackening the soil surface) and/or the creation of an ash layer by a fire are usually quite obvious and their ability to affect the thermal regime of a fire-affected soil can almost be taken for granted. In general, when the soil surface is blackened the surface albedo is reduced (Beringer *et al.* 2003), which will increase the surface forcing, the surface amplitudes of the temperature and soil heat flux, associated with the otherwise normal ambient environmental heating and cooling of the soil. But the presence of an ash layer will tend to compensate somewhat for this additional soil forcing because it will insulate the soil beneath it from the enhanced heating.

On the other hand, changes in the soil thermal properties, the soil volumetric specific heat (C_s, a measure of a soil's ability to store heat) and the soil thermal conductivity (λ_s, a measure a soil's ability to conduct heat), are much less obvious, but they are no less significant because they are coupled directly to many of the other fire-induced changes in the soil. For example, changes in λ_s are likely to imply changes in soil structure because λ_s is so strongly determined by soil structure (Farouki 1986). In addition, changes in C_s, which is closely tied to soil composition (e.g. DeVries 1963; Campbell and Norman 1998), are likely to occur whenever soil organic matter is combusted or soil bulk density changes. Consequently, given the range of possible impacts that fire can have on soils it would be rather surprising not to expect some change in the soil thermal properties as a result of fire.

This study (*a*) examines post-fire changes in λ_s and C_s and changes to the daily and annual variations in soil surface temperature caused by prescribed experimental slash pile burns at two sites in the Rocky Mountains of central Colorado and (*b*) explores the consequences these changes may have to the long-term thermal regime of the soil at these sites. Knowledge of λ_s and C_s is necessary because they essentially determine how deeply naturally occurring heat pulses penetrate the soil (Campbell and Norman 1998).

The present study is unique in several ways: (*i*) It demonstrates that severe soil heating, common during a prescribed burn, can have a significant impact on soil thermal conductivity. (*ii*) It suggests that such impact has long-lasting consequences to the soil thermal regime to significant depths in the soil. (*iii*) Direct in situ measurements of the soil thermal properties indicate (at least for this soil during typical climatic conditions) that λ_s and C_s increase linearly with depth, which is quite different than normally assumed when modeling soil heat flow. (*iv*) It includes the first measurements of the thermal properties of ash. (*v*) The study includes a soil heat flow model (unique in itself) and a model/data synthesis intended to extend the present findings beyond the temporal and spatial limitations of the observed data.

This fifth (unique) feature is essential to fully demonstrate the potential impacts that fire may have on the thermal regime of soils. Specifically, we develop and use a model, rather than using observed soil temperatures, to more easily isolate and highlight the effects that the observed changes to the soil's thermal properties can have on the soil's thermal climate. Otherwise a purely observationally-based or soil-temperature-based study of the post-fire soil thermal climate will necessarily be complicated by the fire's impact (if any) on the long-term soil moisture and its interactions with different types of solar and environmental forcing. Additionally, the model–data fusion component of this study is also intended to provide guidance for and assistance to ongoing and future research into how and how fast soil microbial and plant life recover in such thermally altered environments.

Although aspects of the present study are unique, it is not the first to investigate changes in thermal properties of soils that may result from soil heating during prescribed burns. Massman and Frank (2004) attempted to infer changes in λ_s and C_s indirectly by seeking measurable changes in the vertical profiles of the daily soil temperature and heat flux cycles obtained 2–3 months before and after a burn. The present study employs direct measurements of the vertical profiles of λ_s and C_s, which is very different from Massman and Frank (2004). In addition the present study is more focused on the long-term post-fire soil thermal regime, whereas Massman and Frank (2004) were more concerned with soil heating during the fire and somewhat shorter term changes in the soil. Nor is the present study the first to make in situ measurements of a soil's thermal conductivity. Wierenga *et al.* (1969) employed a similar method for their determinations of λ_s. Nevertheless, Wierenga *et al.* (1969) do not discuss any possible vertical structure of λ_s they may have observed. Nor do they attempt to explicitly model the relationship between λ_s and soil moisture, even though their study was focused on the impact that irrigation can have on soil heat flow. Finally, the present study is not the first to investigate soil temperatures after a prescribed burn. For example, Iverson and Hutchinson (2002) showed that the daily maximum soil temperatures (at 0.01 and 0.02-m depths) at several different prescribed burn sites can remain elevated by more than 10°C over the non-burn control sites for six months after a burn. Although this earlier study focused on (relatively) shorter term and shallower depths than the present study, the authors are clearly of a similar mind with the present study when they speculate that any fire-induced change to the soil's thermal regime could potentially have significant ecological consequences.

The remainder of this study is divided into four parts. The next section describes the site, its soil, the two experimental burns, and the methods used for obtaining the observed data. The following section presents the observational results. The *Implications* section and the Appendix describe the soil heat flow model used to simulate the soil thermal regime before and after the burns and explores the nature of the changes induced in the day-to-day temperature variations in the soil caused by the fire. The final section summarises the conclusions of this study.

Methods

Overview of the site, soils, and experimental burns

All data reported here were obtained at Manitou Experimental Forest (MEF: 39°04′N and 105°04′W), in the central Rocky Mountains about 45 km west of Colorado Springs, Colorado, USA. MEF has a mean elevation of about 2400 m above sea

level, an annual mean temperature of about 5°C, and an annual mean precipitation of about 400 mm. The vegetation within the experimental forest is savanna-like dominated by a ponderosa pine (*Pinus ponderosa*) overstory with a mixed understory of bunchgrasses, forbs, and shrubs, including some non-native invasives. Soils within MEF tend to have low available water holding capacity, moderately high permeability, and bulk densities that typically range between 1.2 and 1.7 Mg m^{-3}. The dominant parent materials of the soils in this region are primarily Pikes Peak granite and secondarily weathered red arkostic sandstone. Fairly detailed descriptions of the soils throughout MEF can be found in Retzer (1949) and the US Department of Agriculture (1986).

To date three experimental burns have been performed at MEF. All burns sites were instrumented, at a minimum, with an array of thermocouples to measure vertical profiles of soil temperature before, during, and after the burns. The same logistical procedures were followed for each of the experimental burns. After a site was selected, it was then instrumented and finally the slash pile was constructed either manually or mechanically over the area. All wires and cables connecting the instruments to the data loggers were buried after installation. All soil samples and soil pits used for determining soil properties were located either within a burn-scarred area (for fire-affected soils) or at a nearby area that clearly had not been affected by a burn (untreated control soils).

The first burn occured during January 2002 and is described in detail by Massman *et al.* (2003) and Massman and Frank (2004). Soils within this burn area are Pendant cobbly loam with a bulk density of about 1.3 ± 0.3 g cm^{-3} and a porosity of about 0.50 ± 0.08. These soils are either sandy clay loams or sandy loams composed of about 60% sand, 25% silt, and 15% clay. Soil organic material comprised about 1–2% of the soil by volume. Soils beneath and immediately surrounding this burn area tend to be denser than those at the other burn sites, a consequence, we hypothesise, of the compaction that likely occured during a period (at least 30 years prior) when the area was used as an access road to other parts of the experimental forest. Although the compaction issue itself is only of secondary concern to the present study (see below), we should note that compaction of soils can affect more than just soil thermal properties with many (non-thermal) consequences to roots and soil microbial biota (e.g. Tan *et al.* 2005; Page-Dumroese *et al.* 2006).

The second burn occured during April 2004. The site of this burn is heavily instrumented for vertical profiles of soil temperature, heat flux, moisture, and CO_2 (Massman *et al.* 2006). This sensor array is replicated at the center and edge of the treatment or burn plot and at two control plots. The soil within the treatment and control areas is a deep (>1.0 m), fine-loamy, mixed, frigid, Pachic Argiustoll and is typical of soils throughout this experimental area. Soils within this particular area are approximately 66% sand, 21% silt, and 13% clay with bulk densities that usually increase with depth and range between 1.1 and 1.5 Mg m^{-3}. Soil organic material comprises about 1–2% of the soil by volume. Previous grazing and mechanical harvesting throughout the area has resulted in a moderately disturbed soil.

The third and last burn, which occured during November 2004, generated much more ash than the other two burns. The only relevance this fire has to the present study is that it provided the ash samples used to determine the thermal properties of ash (discussed later). Consequently, no other details will be discussed here concerning either this burn or the site at which it occured.

Soil thermal properties

Profiles of λ_s [W m^{-1} K^{-1}] were obtained during April 2005 at the second burn site and during September 2005 at first burn site. These sampling periods were about 3.75 years after the first burn and about 1 year after the second. By this time the vegetation had recovered at the first burn site, but the second burn area was virtually free of vegetation and still discolored (black in color). Each of the thermal conductivity measurements were acquired in situ using a 0.06 m long single heated-needle conductivity probe (East 30 Sensors; Pullman, WA, USA) (e.g. Wierenga *et al.* 1969; Bristow 2002) by inserting the probe horizontally into the side of a freshly dug pit, which was usually about 0.3 m deep, 0.3 m wide, and 0.5 m long. Vertical profiles of λ_s were obtained by sequentially sampling at 0.02, 0.05, 0.10, 0.15, and 0.20-m depths with the same probe for two different sides of each pit. During the 2 to 5 min the probe required to thermally equilibrate, the pit was covered with an large piece of Styrofoam (commercially available household insulator) to minimise any external heating of the sides of the pit by solar radiation.

Coincident with these profiles of λ_s are profiles of volumetric soil moisture, θ_v [m^3 m^{-3}], and bulk density, ρ_b [Mg m^{-3}]. Profile data for θ_v are necessary because soil moisture is the major determinant of λ_s (Farouki 1986; Campbell and Norman 1998). After soil moisture, soil structure has the most important affect on λ_s, but because the term 'soil structure' is more descriptive than quantifiable ρ_b is often used instead (Farouki 1986; Jury *et al.* 1991). Broadly speaking, regardless of soil type λ_s is a monotonically increasing function of both θ_v and ρ_b; but the rate of increase is dependent upon soil type (e.g. Farouki 1986; Campbell and Norman 1998).

Bulk density and gravimetric soil moisture measurements were obtained by weighing and drying soil samples taken near each pit using an AMS split-core sampler (12″ length (0.30 m), 2″ diameter (0.05 m)) with a core tip (Forestry Suppliers; Jackson, MS, USA). Each soil core was subsampled for a vertical profile every 0.05 m with depths centered at 0.05, 0.10, 0.15, and 0.20 m. All soil samples were extracted from the corer, placed in soil tins, and brought back to the Rocky Mountain Research Station for analysis.

At the first burn site a total of 13 pits were dug: 4 within the burned area itself; 3 controls near – but outside – the burn area, which we could not clearly identify as having been used as the access road; 3 in a nearby unburned area, which we could identify as having been used as a road; and 3 in nearby areas which we could clearly identify as having never been driven on or otherwise significantly disturbed. At the second site a total of 9 pits were dug: 3 in the center of the burned area, 3 at the edge of the burned area, and 3 near the control sites.

A split-core sampler was also used to obtain soil samples for the determination of soil specific heat capacity, c_s [J g^{-1} K^{-1}], which combined with the relationship $C_s = \rho_b c_s$ are used to obtain C_s [MJ m^{-3} K^{-1}]. After drying the samples, all c_s measurements were made at Thermophysical Properties Research

Laboratory (West Lafayette, IN, USA) with a Perkin-Elmer model DSC-2 (Differential Scanning Calorimeter) with sapphire as a reference material. These laboratory analyses focused on determining the relationship between dry c_s and temperature T [°C or K], which is usually well approximated by a linearly increasing function (e.g. Kay and Goit 1975). For studies of soil heating during fires knowledge of this functional dependence, $c_s(T)$ or $C_s(T)$, is important because the soil temperatures may increase by several hundred °C during a fire. But the daily or annual variations in soil temperature, being 10 to 40°C, have much less impact on c_s or C_s. Details concerning this temperature dependency are examined in the Appendix.

The laboratory-based approach for obtaining estimates of c_s imposed some significant logistical constraints on the sampling strategy for c_s. The c_s samples were obtained from the same soil cores as the bulk density samples, which were physically larger sample volumes than employed with the field determinations of λ_s. Consequently, it was not possible to obtain the same vertical resolution for c_s that we could with λ_s. We obtained 5 c_s samples within the fire affected areas at the two burn sites and 17 c_s samples at various non-burn locations within the general region encompassing the two sites. At the first burn site the soil samples were obtained with aluminum cylinders that were 0.051 m in diameter and 0.152 m long. Such soil cores mean that the c_s values obtained at the first burn site were average values representative of the first 6 inches (15.2 cm) of soil. At the second burn site the soil cores were subsampled to obtain measurements of c_s between 0 and 0.127 m (5 inches) and between 0.127 and 0.254-m depth. Although c_s is undersampled compared to λ_s, any potential limitations associated with this undersampling are largely overcome by combining a simple physically-based model of C_s with the observed vertical profiles of ρ_b (see Appendix).

Thermophysical Properties Research Laboratory also performed an analysis for λ_s on soil samples matched with each of the c_s samples. After oven-drying the samples λ_s was determined with the heated probe method over a range of temperatures. As with c_s, λ_s is also temperature dependent (e.g. Campbell *et al.* 1994; Massman and Frank 2004), but as shown in the Appendix, these affects can be ignored for the purposes of the present study. Nevertheless, the laboratory determinations of λ_s near normal soil temperatures are used to confirm the field-based results concerning fire's impact on λ_s.

Data analyses primarily employed the multiple regression software subroutine SAS PROC GLM (part of the software package SAS 9.1 for Windows) (SAS Institute, Cary, NC, USA) and secondarily SAS PROC REG, MIXED, and TTEST.

Ash thermal properties

Measurement procedures for the thermal properties of ash were similar to those discussed in the preceeding section for C_s and λ_s. Sampling differences were (*i*) λ_{ash} determinations were made within the top 0.06 m of any ash pile, (*ii*) no laboratory determinations of λ_{ash} were made, and (*iii*) the field determinations of λ_{ash} were made 32 different locations within the burn area, where 16 of these locations are characterised as 'shallow' ash piles and 16 as 'deep' ash piles. Five samples were obtained for the analysis of C_{ash} using a trowel rather than a soil corer. Ash bulk density, ρ_{ash}, and moisture, θ_{ash}, samples were taken to coincide with the λ_{ash} samples.

Soil surface temperature

All soil and soil surface temperatures were measured with thermocouples (Omega Engineering, Stamford, CT, USA). To insure electrical isolation all thermocouple junctions were coated with epoxy (Omegabond 101 or Omegabond 200 for high temperature exposures) prior to insertion into the soil.

Results

Soil temperatures during the experimental burns

Fig. 1 is a picture of the first burn pile and Fig. 2 shows the soil heating during the first burn. Similarly, Figs 3 and 4 show the second burn pile and the soil heating during the second burn. We present this information because soil temperatures during a burn can be used to characterise threshold values at which one may expect changes in soil biota, soil chemistry, and soil minerals (Neary *et al.* 2005). We note in passing (*i*) there were no soil surface temperature measurements were made during the first burn and (*ii*) that although the fuel loading is considerably higher with the second burn than the first (see figure captions), the duration of the soil heating and the maximum soil temperatures were actually greater with the first burn. The reason for this reversal of the expected soil heating pattern is not known, but is likely to be related to the difference in soil thermal properties (due to the compaction and higher soil bulk densities at the first burn site) as well as to the geometric structure of the piles and the dynamics of the combustion event itself.

Soil bulk density

Variations in ρ_b were sought in the measured bulk density data set ($n = 92$) using burn site, treatment, and depth. The final model, valid for $0.025 \leq z \leq 0.20$ m, yielded:

$$\rho_b(z) = 1.4 + 1.18z \quad \text{[Site 1]}$$
$$\rho_b(z) = 1.2 + 1.18z \quad \text{[Site 2]}$$

where z is soil depth [m], which is taken as positive downward from the surface. The model Root Mean Square Error $= 0.127\ \text{Mg m}^{-3}$, its $R^2 = 0.504$, and its significance, $P < 0.0001$.

Conclusions from this analysis are that (*i*) the burns themselves did not cause any statistically significant changes in soil bulk density ($P = 0.62$), (*ii*) the bulk densities at these two sites increase with depth ($P < 0.0001$), and (*iii*) soils at the first site are denser than at the second ($P < 0.0001$). This first conclusion probably should not be too surprising, given that soil organic matter is so low, less than 2% by volume in MEF soils. Consequently, eliminating soil organic matter by burning it will have very little affect on the bulk composition of the soil.

The differences in bulk density between sites, as related to the third conclusion, were further examined using the ρ_b data from the first site obtained from the soil pits in areas that could clearly be identified as being either road or undisturbed. The results indicate that only the bulk densities within the top 0.05 m of clearly undisturbed soil were less than ($P = 0.0013$) any other densities

Fig. 1. Manually-constructed slash pile for the first experimental burn. Fuel loading is estimated to be between 250 and 300 kg m^{-2}.

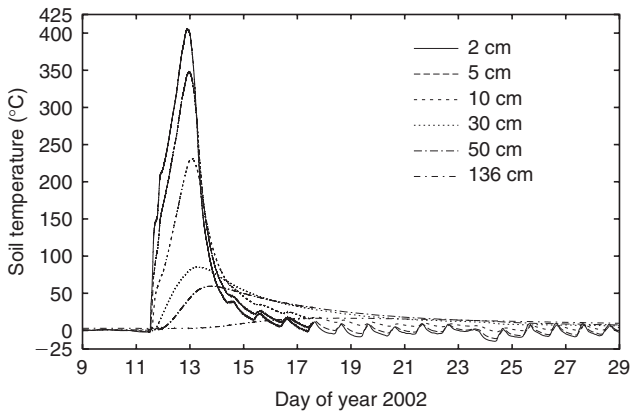

Fig. 2. Measured soil temperatures beneath the center of the first slash pile (Fig. 1) before, during, and after the prescribed burn. The burn was initiated about noon on January 11. The maximum soil temperature at 0.02 m was 400°C.

measured at 0.05 m. But, because the soil density profiles below 0.05 m are not statistically different, it is likely that any compaction effects are limited to the upper 0.05 m only. Although we cannot prove it, we suggest that the upper 0.05 m of soil was compacted years earlier during logging operations at this site.

Finally, we note that there were no statistically significant differences between the bulk densities at the center and edge of the burn area at the second site.

Soil thermal properties

The thermal conductivity data set was first tested in a manner similar to that for bulk density and we found that it tended to increase with depth at both burn sites, confirming our previous results at the first burn site (Massman and Frank 2004), at which we inferred the depth dependency of the thermal properties by examining the time lag between measured soil heat fluxes and soil temperatures (e.g. Massman 1993).

Nevertheless, a more appropriate model of λ_s is one that explicitly includes the effects of bulk density and soil moisture as independent variables and that does not explicitly include soil depth. In general, the functions used to describe $\lambda_s = \lambda_s(\rho_b, \theta_v)$ are nonlinear (e.g. Farouki 1986; Hopmans and Dane 1986; Campbell and Norman 1998). For the purposes of this study, which is focused mostly on possible change in λ_s as a result of fire, we choose the simplest model possible. The regression model we used is $\lambda_s = A\rho_b + B\theta_v$. The results, given next, are valid for $0.01 \le \theta_v \le 0.23$ m^3 m^{-3} and $1.05 \le \rho_b \le 1.75$ Mg m^{-3} and are the same for both the first and second sites ($n = 108$, with a model $R^2 = 0.428$, Root Mean Square Error $= 0.259$ W m^{-1} K^{-1}, and $P < 0.0001$ for the model and all parameters).

$$\lambda_s = 0.123\rho_b + 8.21\theta_v \quad \text{[All non-fire-heated soils]}$$
$$\lambda_s = 0.486\rho_b + 2.70\theta_v \quad \text{[All fire-heated soils]}$$

Fig. 5 shows a three-dimensional plot of these two relationships with the observed data. Results indicate that for dry soils

Fig. 3. Mechanically-constructed slash pile for the second experimental burn. Fuel loading is estimated to be between 450 and 600 kg m^{-2}.

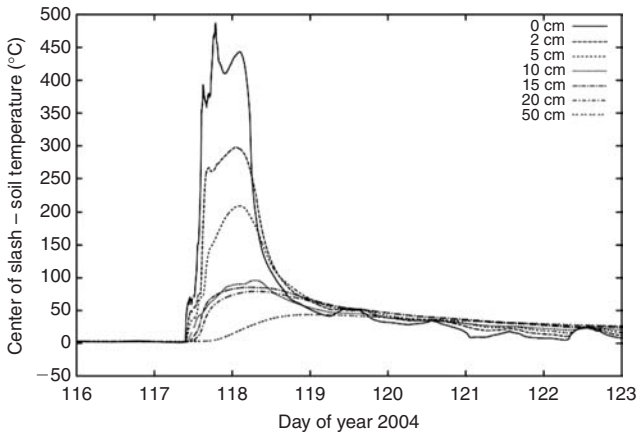

Fig. 4. Measured soil temperatures beneath the center of the second slash pile (Fig. 3) before, during, and after the prescribed burn. The burn was initiated in the early afternoon on April 26. The maximum soil temperature at 0.02 m was 300°C.

($\theta_v < \sim 0.1$), λ_s has increased as a result of the soil heating during the burn; whereas, for moist soils ($\theta_v > \sim 0.1$) λ_s has decreased as a result of the soil heating during the burn.

These last two relationships indicate that λ_s has changed as a result of the fire. Nevertheless, the nature of the change is a bit surprising. Both sites show that thermal conductivity is about four times more sensitive to bulk density after the burn than before. While λ_s appears to be about one-third as sensitive to soil moisture after the fire than before. This factor of four change in sensitivity of λ_s to ρ_b ($d\lambda_s/d\rho_b = A$) is consistent with the factor of 2.8 increase in λ_s observed by Thermophysical Properties Research Laboratory in dry fire-heated soils relative to dry non-fire-heated soils (see Appendix). Maybe even more startling is λ_s's reduction in sensitivity to soil moisture ($d\lambda_s/d\theta_v = B$), which might be likened to changing a sandy soil to a clayey soil (e.g. Campbell and Norman 1998) as a consequence of the soil heating during the fire. Such a change did not occur to the soils at our experimental burns; nonetheless, these results do suggest some change in soil structure as a result of the burns. Unfortunately, the nature of this change is not clear from this particular data set.

The present results clearly differ from those of Massman and Frank (2004), who did not detect any clear fire-induced changes in λ_s during the two months immediately following the first burn. The reason for this contradiction is not known. Nonetheless we can conceive of several possible explanations, each involving some aspect of poor or inadequate contact between the soil and the heat flux plates, which Massman and Frank (2004) speculate is a contributing factor to the difference between their field-based estimates of λ_s and those obtained in a laboratory. Poor soil–plate contact increases the contact resistance of the plate, in turn biasing the soil heat flux measurements and the associated estimates of λ_s. It is possible, therefore, that inadequate contact may generally render the model-based methods Massman and Frank (2004) employed, which depend heavily on the soil heat flux data, too imprecise to observe or quantify any change to λ_s. Or if the structure of the soil did change as a result of the heating during the first burn, then it is possible the nature of the contact between the heat flux plates and the soil may also have changed in

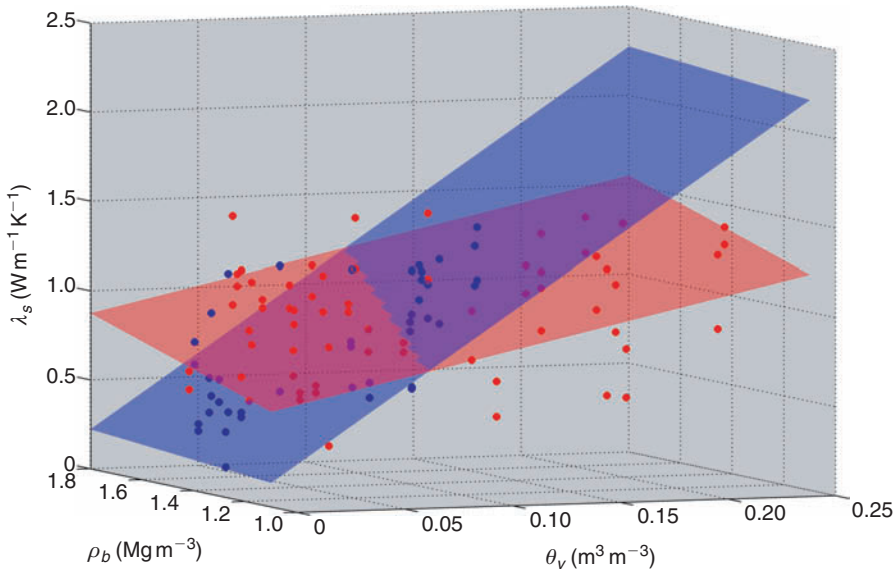

Fig. 5. 3-Dimensional plot of the measured soil thermal conductivity, λ_s, as a function of soil bulk density, ρ_b, and soil volumetric water content, θ_v, for all burn area and non-burn area data (red and blue dots). Also shown are the linear regression relationships (red and blue planes) showing $\lambda_s = \lambda_s(\rho_b, \theta_v)$. The regression relationships indicate that for dry soils ($\theta_v < \sim 0.1$), λ_s has increased as a result of the soil heating during the burn; whereas, for moist soils ($\theta_v > \sim 0.1$) λ_s has decreased as a result of the soil heating during the burn.

such a way that Massman and Frank (2004) could not detect any change in λ_s. Finally, it may also be possible that the change in λ_s did not occur until after the observations of Massman and Frank (2004). If this is the case, then one might speculate that the fire-induced changes in the soil structure may have been facilitated by (or required) the mechanical expansion and contraction of the soil that occurs during thaw-freeze cycles. Such a mechanical perturbation to the soil would have the potential to alter the soil structure, as well as the contact between the soil and the plates.

Samples from the burn and non-burn areas were analysed for fire-induced changes in dry c_s by linearly regressing the laboratory values of $c_s(T)$ against temperature, i.e., $c_s(T) = c_{s0} + \Delta_{cT} T$. Over the range of temperatures between 23 and 100°C, which is most relevant to this study, the results show no statistically significant differences between the burn and non-burn samples ($P = 0.1516$). For this temperature range and a dry soil, $c_s(T) = 0.72 + 0.002T$ [J g^{-1} K^{-1}], where T is °C, and the model $R^2 = 0.863$, its Root Mean Square Error = 0.0193 J g^{-1} K^{-1} and $P < 0.0001$. Other measurements of $c_s(T)$ were also made between 23 and 300°C. Over this temperature range the slope, Δ_{cT} [J g^{-1} K^{-1} °C^{-1}], of the burn area soils was greater ($P < 0.0001$) than for the non-burn areas. Whereas the intercept, c_{s0} [J g^{-1} K^{-1}], was the same for both. Although the evidence over this wider temperature suggests a statistically significant change in Δ_{cT}, the increase is only 13%, which is unlikely to be important for most practical considerations. We conclude that dry soil specific heat (c_s) for most MEF soils is unlikely to be directly affected by fire and because ρ_b was not affected by the fire, it follows that C_s is also unaffected by the fire. Nevertheless, fire can indirectly affect dry c_s and C_s through the temperature term $\Delta_{cT} T$ providing the surface forcing amplitudes of the daily and annual cycles of soil temperature change as a result of fire.

Thermal properties of the ash layer

Measurements of the bulk density of ash, ρ_{ash}, at MEF indicate that $\rho_{ash} = 0.96 \pm 0.24$ Mg m^{-3} (mean ± standard deviation). Differences between samples as related to ash layer depth were not statistically significant. Because the structure and depth of the ash layers made it very difficult to study the vertical stratification of ash bulk density, we assume that ρ_{ash} is uniform with depth.

Measurements of the thermal conductivity of ash, λ_{ash}, revealed that λ_{ash} is a function of volumetric ash moisture, $\theta_{v,ash}$. Following the approach outlined for λ_s discussed in the previous section, the final regression relationship between λ_{ash}, ρ_{ash}, and $\theta_{v,ash}$, is $\lambda_{ash} = 0.098\rho_{ash} + 5.68\theta_{v,ash} = \lambda_{0,ash} + 5.68\theta_{v,ash}$, for the range $0.003 \le \theta_{v,ash} \le 0.048$; where $\lambda_{0,ash} = 0.094$ W m^{-1} K^{-1} and the model $R^2 = 0.36$, its Root Mean Square Error = 0.148 W m^{-1} K^{-1}, and $P < 0.0001$.

Finally, the specific heat of dry ash was found to be $c_{ash} = 0.71 + \Delta_{cT,ash} T$ [J g^{-1} K^{-1}], where $\Delta_{cT,ash} = 0.0018$ J g^{-1} K^{-1} °C^{-1}. Here we note that $c_{ash}(T) \approx c_s(T)$, suggesting that any ash remaining after complete combustion of the wood is likely to be composed largely of the soil minerals incorporated into the wood as the tree was growing. The rather small difference between $c_{ash}(T)$ and $c_s(T)$ may be a consequence of the loss (by combustion) of the organic matter in the c_{ash} samples that the c_s samples would have retained. Combining these results with the ρ_{ash} and $\theta_{v,ash}$ yields $C_{ash} = C_{0,ash} + C_w\theta_{v,ash}$, where $C_{0,ash} = 0.73 \pm 0.21$ MJ m^{-3} K^{-1} and C_w is the volumetric specific heat capacity of water. Note that the weak temperature

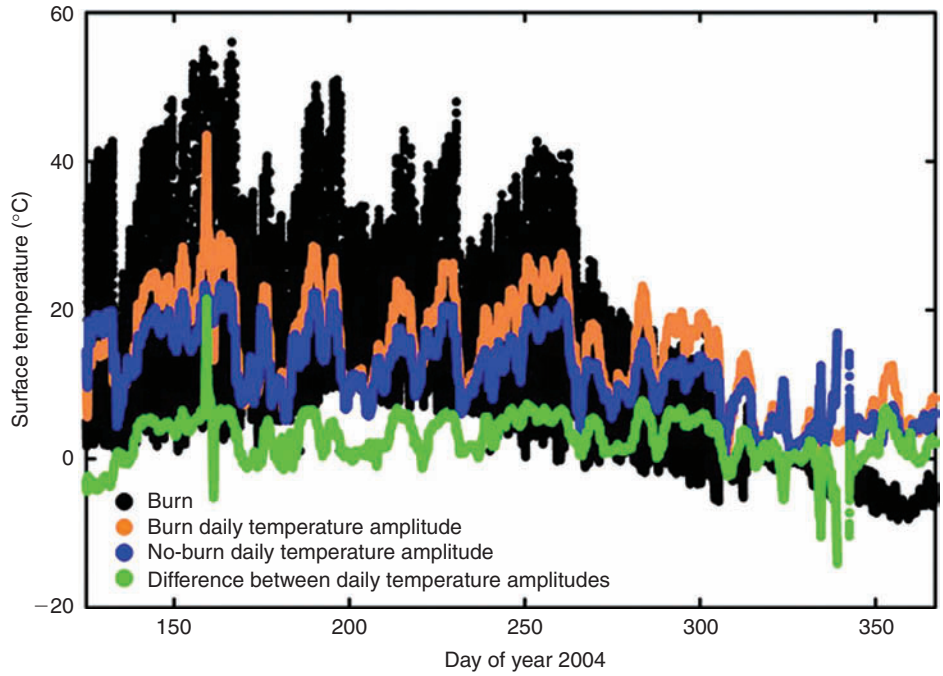

Fig. 6. Time course of (*i*) soil surface temperature at the burn area and (*ii*) the difference in soil surface temperatures associated with the daily cycle of solar heating between the burn area and the non-burn control area from June through mid-December 2004. Also included are the soil surface temperatures associated with the daily cycle of solar heating at both the burn area and the non-burn control area, as obtained from the full data set by band-pass filtering.

dependency reflected by $\Delta_{cT,ash}$ has been subsumed into $C_{0,ash}$ and its associated uncertainty.

Soil surface temperature

Fig. 6 shows the amplitude of the daily temperature cycle of solar heating for the center of the 2004-burn area as well as the control for June through mid December 2004. Fig. 7 shows the amplitude of the annual temperature cycle of solar heating at the same areas for the same period. These cycles were isolated by applying appropriate filters to the original time series. Figs 6 and 7 also show the difference (burn minus control) in the amplitudes of the surface temperature. These two figures also include the observed surface temperatures for the burn area. In both cases the amplitude associated with the periodic heating of the soils is higher at the burn location than at the control. For daily heating the amplitude difference can reach nearly 8°C, whereas the difference in the annual cycle is about 2°C. These temperature differences are large and represent a significant increase in surface forcing on both the daily and annual cycles of soil heating. Nevertheless, they are realistic and quite similar to the differences in the daily maximum temperatures of soils caused by prescribed burns that were observed by Iverson and Hutchinson (2002). Furthermore, these figures include only average conditions, they do not include the temperature variations associated with synoptic scale weather (with periods between 3 and 10 days) or the forcing associated with cloudiness or thunderstorms (with periods of a few minutes to a few hours). Consequently, on any given day the difference between the surface temperature maxima at these two locations can sometimes exceed 15°C. It should not be surprising that such large daily and seasonal temperature differences can extend to significant depths of the burn area soil (e.g. Hungerford and Babbitt 1987). But, as discussed in the following section, the impact that these surface temperature differences can have at difference soil depths can be either enhanced or suppressed depending on the changes to the soil thermal properties.

Implications to the soil thermal regime

The preceeding sections have outlined how the soils at MEF have been altered as a result of fire. Both the soil thermal conductivity and the thermal forcing at the soil surface (and to a much lesser extent the soil specific heat capacity) have changed as a consequence of the heating during the prescribed burns. This section examines and synthesises the consequences of these changes using a model of the daily and annual cycles of soil heating.

There are three important considerations concerning the model as developed here that need to be emphasised. First, we seek to keep the modeling as simple as possible, but at the same time remaining as faithful to the observations as possible. So this section begins with the development of mathematical relationships that explicitly account for the depth dependency of ρ_b, θ_v, λ_s, and C_s. Second, the model formulations for the soil thermal properties do not explicitly include any temperature affects, although the measured values themselves do. The Appendix discusses and quantifies this additional dependency in some detail for both λ_s and C_s. The nature of this issue is made more apparent below. But the basic purpose of the model formulation and all

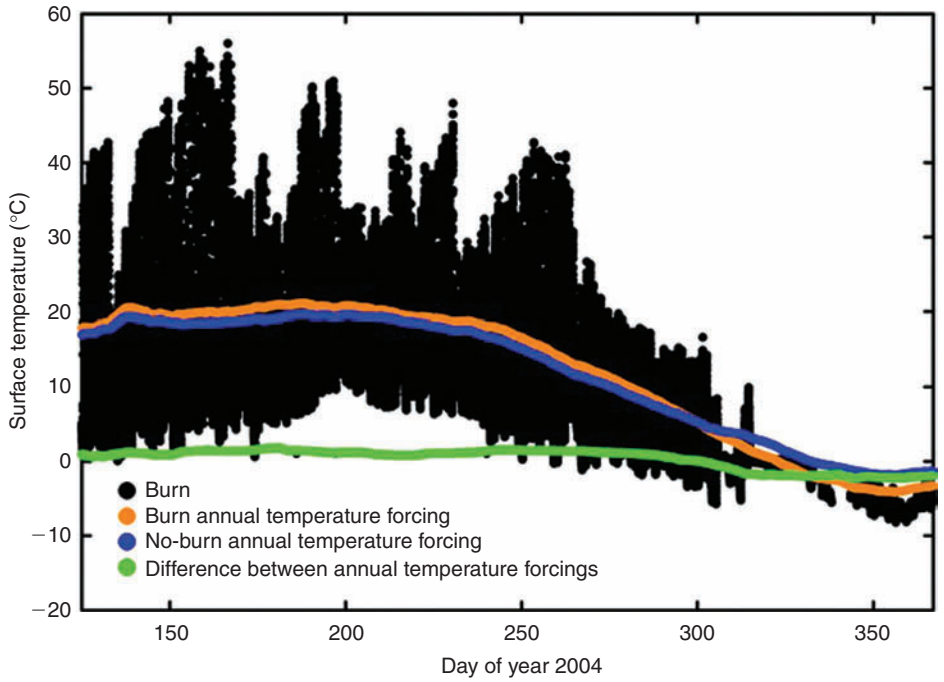

Fig. 7. Time course of (*i*) soil surface temperature at the burn area and (*ii*) the difference in soil surface temperatures associated with the annual cycle of solar heating between the burn area and the non-burn control area from June through mid-December 2004. Also included are the soil surface temperatures associated with the annual cycle of solar heating at both the burn area and the non-burn control area, as obtained from the full data set by low-pass filtering.

related approximations is to eliminate several small nonlinearities caused by this temperature dependency, and thereby allow an analytical solution to the soil heat flow equation for the case of periodic thermal forcing at the soil surface. Third, augmenting the model with an ash layer is also intended to be simple and any impact that an ash layer will have on the long-term thermal regime of the soil will depend on factors that influence the ash layer's stability and erodibility. But, these issues are beyond the intention of the present study.

The vertical structure of the soil's thermal properties

To develop a model of $\lambda_s = \lambda_s(z)$ requires a model for $\theta_v(z)$, which can then be combined with the model for $\lambda_s = A\rho_b(z) + B\theta_v(z)$ and the model $\rho_b(z) = \rho_{b0} + \alpha_\rho z$. Again with the intent of keeping all models as simple as possible, the soil moisture data coincident with our measurements of λ_s suggests that a linearly increasing model, i.e., $\theta(z) = \theta_0 + \alpha_\theta z$ with $\alpha_\theta > 0$, is an adequate model for describing the vertical distribution of soil moisture ($P < 0.0001$). The final model for $\lambda_s(z)$ is

$$\lambda_s(z) = \lambda_0(1 + \alpha_\lambda z) \quad 0.025 \le z \le 0.20\,\text{m} \tag{1}$$

where

$$\lambda_0 = A\rho_{b0} + B\theta_0 \tag{2}$$

and

$$\alpha_\lambda = \frac{A\alpha_\rho + B\alpha_\theta}{\lambda_0} \tag{3}$$

The model for $C_s = C_s(z)$ is similar to Eqn 1, but requires combining the models for $\rho_b(z)$ and $\theta_v(z)$ with the model for $c_s = c_s(T)$ along with some additional preliminary development and justification.

C_s is explicitly determined by the specific heat capacities of its constituents: minerals, organic matter, water, and air (e.g. DeVries 1963; Jury *et al.* 1991).

$$C_s = \phi_m C_m + \phi_o C_o + \theta C_w + \phi_a C_a \tag{4}$$

where ϕ is the volume fraction for minerals (ϕ_m), organic matter (ϕ_o), air (ϕ_a), and θ is the volumetric soil moisture, and C is the volumetric specific heat for a given constituent (the subscript has been dropped for convenience). [Recall that $C = \rho c$ where ρ is the density of the material and c is the specific heat capacity of the material.] The soil air term, $\phi_a C_a$, is about three orders of magnitude smaller than either of the first two terms and can safely be ignored. Furthermore, because MEF soils are almost 100% mineral soils (typically $\phi_o \le 0.02$), it is reasonable to assume that $c_m = c_s$ and that contributions from the soil organic component can be ignored. Employing these approximations and after some mathematical manipulation, Eqn 4 can be expressed as

$$C_s(z, T) = \rho_b(z)c_s(T) + \theta(z)C_w(T) \tag{5}$$

To eliminate the implicit depth dependency associated with temperature (see Appendix concerning this nonlinearity) we now assume that $c_s(T)$ can written as $c_s = c_{s0} = 0.72 + \Delta_c\overline{T}(0)$,

where $\overline{T}(0)$ is the mean soil surface temperature. Note that $\overline{T}(0)$ is not necessarily the same for the burn and control areas, nor does it take on the same value for the daily soil temperature cycle as it does for the annual cycle. C_w is also a function of temperature and so it is included as such in Eqn 5. Specifically, $C_w(T) \approx 4.216 + \Delta_{wT} T$ [MJ m^{-3} K^{-1}] (e.g. Wagner and Pruss 2002), where the temperature coefficient $\Delta_{wT} = -0.0017$ [MJ m^{-3} K^{-1} °C^{-1}] < 0, largely because the density of water decreases as temperature increases. As with c_s we will approximate $C_w(T)$ so that $C_w = 4.216 + \Delta_{wT}\overline{T}(0)$. The final model for $C_s(z)$ is

$$C_s(z) = C_0[1 + \alpha_c z] \quad 0.025 \le z \le 0.20\,\text{m} \tag{6}$$

where

$$C_0 = \rho_{b0} c_{s0} + C_w \theta_0 \tag{7}$$

and

$$\alpha_c = \frac{c_{s0}\alpha_\rho + C_w \alpha_\theta}{C_0} \tag{8}$$

and

$$c_{s0} = 0.72 + \Delta_{cT}\overline{T}(0) \tag{9}$$

and

$$C_w = 4.216 + \Delta_{wT}\overline{T}(0) \tag{10}$$

A model of the daily and annual cycles of soil heating

This study models soil heat flow in a layered soil using analytical solutions to

$$C_s(z)\frac{\partial T}{\partial t} = \frac{\partial}{\partial z}\left(\lambda_s(z)\frac{\partial T}{\partial z}\right) \tag{11}$$

under the assumptions that $C_s(z) = C_0(1 + \alpha_c z)$ and $\lambda_s(z) = \lambda_0(1 + \alpha_\lambda z)$ in the upper layer and that $C_s(z)$ and $\lambda_s(z)$ are uniform with depth in the lower layer. The model assumes that $\alpha_c \neq \alpha_\lambda$, and that the forcing (upper boundary condition) is periodic in time: $T(0, t) = \overline{T}(0) + A_T(0)e^{i\omega t}$; where $A_T(0)$ is the amplitude of the daily or annual surface temperature forcing and the overbar indicates the mean or steady-state temperature, ω is the frequency of the periodic forcing, t is time, and $i = \sqrt{-1}$. We begin the model development with the upper layer.

Assuming the solution to Eqn 11 is $T(z, t) = \overline{T}(z) + A_T(z)e^{i\omega t}$ and making the substitutions for $C_s(z)$ and $\lambda_s(z)$, yields two differential equations:

$$\frac{d}{dz}\left(\lambda_s(z)\frac{d\overline{T}(z)}{dz}\right) = 0 \tag{12}$$

$$\lambda_0(1 + \alpha_\lambda z)\frac{d^2 A_T(z)}{dz^2} + \lambda_0\alpha_\lambda\frac{dA_T(z)}{dz} - i\omega C_0(1 + \alpha_c z)A_T(z) = 0 \tag{13}$$

The solution to Eqn 12 is

$$\overline{T}(z) = -\frac{\overline{G}(0)}{\alpha_\lambda \lambda_0}\ln(1 + \alpha_\lambda z) + \overline{T}(0) \tag{14}$$

where $\overline{G}(0)$ is the time-averaged heat flux at the soil surface. [Recall that $G = -\lambda\partial T/\partial z$.] Note that this solution also implies that $\overline{G}(z) = \overline{G}(0)$ and therefore, that the time-averaged soil heat flux is uniform with depth.

The solution to Eqn 13 largely depends upon the term $(1 + \alpha_c z)$. For example, if $\alpha_c = \alpha_\lambda$ and $1 + \alpha_c z \equiv 1 + \alpha_\lambda z$, the solution is (e.g. Nerpin and Chudnovskii 1984)

$$A_T(z) = pBe(\beta\zeta) + qKe(\beta\zeta) \tag{15}$$

where p and q are constants determined by the boundary conditions; $\beta = \sqrt{\omega C_0/(\alpha_\lambda^2\lambda_0)}$; $\zeta = 1 + \alpha_\lambda z$; $Be(x) = ber(x) + i\,bei(x)$, $Ke(x) = ker(x) + i\,kei(x)$, and $ber(x)$, $bei(x)$, $ker(x)$, and $kei(x)$ are Kelvin functions of order zero (e.g. Spanier and Oldham 1987). A second example of an analytical solution results when $\alpha_c = 0$, or equivalently $1 + \alpha_c z \equiv 1$. The corresponding solution to Eqn 13 for this case is $A_T(z) = pBe(2\beta\sqrt{\zeta}) + qKe(2\beta\sqrt{\zeta})$ (e.g. Andrews 1992).

Unfortunately, no analytical solution exits for the general case $\alpha_c \neq \alpha_\lambda$ with $\alpha_c \neq 0$ and $\alpha_\lambda \neq 0$. Nevertheless, a very good approximation is available by approximating the term $1 + \alpha_c z$ with a non-depth varying constant, which will be denoted henceforth by γ. Therefore, we will replace $1 + \alpha_c z$ with its mean value within the layer $0 \le z \le 0.2$ m. That is $1 + \alpha_c z \approx 1 + 0.5\alpha_c z_m$, where for this study, $z_m = 0.2$ m and $\gamma = 1 + 0.5\alpha_c z_m$. One of the main reasons this is a reasonable approximation is because the range of variation of λ_s tends to exceed that of C_s, or mathematically: $\alpha_c < \alpha_\lambda$ tends to be universally true and $\alpha_c \ll \alpha_\lambda$ is a more likely scenario. As a consequence, there are many occasions when soils can be characterised by $|\alpha_c z| < 1$ or even $|\alpha_c z| \ll 1$. Therefore, approximating $1 + \alpha_c z$ by a constant is not unreasonable because the attenuation of $A_T(z)$ with depth is more strongly influenced by variations in $\lambda_s(z)$ than by variations in $C_s(z)$.

The final model for the daily and annual heat flow in upper portion of MEF soils is

$$A_T(z) = pBe(2\beta\sqrt{\zeta}) + qKe(2\beta\sqrt{\zeta}) \quad 0 \le z \le z_m \tag{16}$$

where $\beta = \sqrt{\omega C_0\gamma/(\alpha_\lambda^2\lambda_0)}$ and p and q can be complex because $Be(x)$ and $Ke(x)$ are complex.

For the lower portion of MEF soils we will assume that the soil thermal properties are uniform with depth, which yields (e.g. van wijk and DeVries 1963; Campbell and Norman 1998)

$$A_T(z) = Qe^{-(1+i)\sqrt{\omega C_m/(2\lambda_m)}\,z} \quad z_m \le z < \infty \tag{17}$$

where C_m and λ_m are thermal properties of this lower layer of soil and Q is a complex constant determined by matching this equation with Eqn 16 at $z = z_m$.

To complete the model requires consideration of two more issues. First, it is also necessary to match the solutions for heat flux, $A_G(z)$, at $z = z_m$. This allows p, q, Q, and $A_G(0)$ to be uniquely determined from the upper boundary condition, $A_T(0)$. The expressions for $A_G(z)$ corresponding to Eqns 16 and 17 are

$$A_G(z) = -\lambda_0\alpha_\lambda\beta\sqrt{\zeta}[pBe'(2\beta\sqrt{\zeta}) + qKe'(2\beta\sqrt{\zeta})] \quad 0 \le z \le z_m \tag{18}$$

and

$$A_G(z) = [\lambda_m(1+i)\sqrt{\omega C_m/(2\lambda_m)}]A_T(z) \quad z_m \le z < \infty \quad (19)$$

where $Be'(x) = dBe(x)/dx$ is the first derivative of $Be(x)$ and similarly for $Ke'(x)$.

Second, we assume that the soil thermal properties are also continuous across the interface at $z = z_m$, i.e., $\lambda_m = \lambda_0(1+\alpha_\lambda z_m)$ and $C_m = C_0(1+\alpha_c z_m)$. This continuity assumption is not mathematically necessary for a layered soil model (e.g. van Wijk and Derksen 1963; Karam 2000), but it does have some consequence to the model and is discussed in greater detail in the next section. There are two aspects of this issue. (*a*) We do not know how deeply the linear profiles of thermal properties extend beyond 0.2 m, but it is quite possible that they can extend beyond 0.2 m. (*b*) Nor do we know how deeply the fire-induced changes in soil thermal properties, and λ_s in particular, penetrate the soil. At some depth the soil heating during the burn should have attenuated sufficiently to preclude any changes to λ_s. Below this level it is unlikely that $\lambda_s = \lambda_m$, contrary to the continuity assumption. For these reasons, any model simulation is necessarily imprecise and we admit to choosing $z_m = 0.2$ and to assuming continuity of the soil thermal properties across z_m as much from ignorance as convenience.

The model does not include a separate layer for ash. Rather we will simply reduce the soil surface temperature amplitude $A_T(0)$, the upper boundary condition on the model, by the factor $\exp(-z_{ash}/D_{ash})$; where z_{ash} [m] is the depth of the ash layer, and D_{ash} [m] is the thermal attenuation depth, i.e., $D_{ash} = \sqrt{2\lambda_{ash}/(\omega C_{ash})}$ (e.g. Campbell and Norman 1998), and λ_{ash} and C_{ash} as discussed above. For daily heating and cooling cycle $D_{ash} = 0.060 \pm 0.006$ m for dry ash ($\theta_{v,ash} = 0$) and $D_{ash} = 0.105 \pm 0.008$ m for moist ash ($\theta_{v,ash} = 0.05$). For the annual cycle $D_{ash} = 1.15 \pm 0.11$ m for a layer of dry ash and $D_{ash} = 2.01 \pm 0.15$ m for a moist layer of ash. The thermal insulating effect that an ash layer with these values of D_{ash} and depth $z_{ash} = 0.05$ m will have on the underlying soil suggests that forcing at the soil surface, $A_T(0)$, will be reduced by approximately 40% to 60% for the daily cycle and between 2 and 4% for the annual cycle. Of course, deeper ash layers will attenuate the soil surface forcing more, while shallower ash layers less.

Before turning to the model simulations, we note that the algorithm we developed for evaluating the Kelvin functions [$ber(x)$, $bei(x)$, $ker(x)$, $kei(x)$] employs relationships or algorithms provided by Whitehead (1911), Spanier and Oldham (1987), and Whyte (1998). Furthermore, for all simulations discussed in the next section the approximate solution provided by Eqn 16 was tested against the numerical solution to Eqn 13 using the thermal wave model developed by Karam (2000). The maximum temperature difference between the numerical and approximate solutions for any simulation was less than 0.3°C, and usually the difference was less than 0.1°C. More precisely, the maximum temperature difference was less than about $0.01A_T(0)$ for all z, and all temperature differences tended to decrease with depth.

How fire alters the post-fire thermal climate of MEF soils

The major effects that fire can have on the long term thermal climate of soils are shown in Figs 8, 9, and 10. All figures include an ash and no-ash simulations and moist and dry ash and soil simulations. Table 1 lists the model input parameters for these simulations. Values of $A_T(0)$ are estimated from Figs 6 and 7. All simulations assume that $\rho_{b0} = 1.2$ Mg m^{-3}, corresponding to the second burn site.

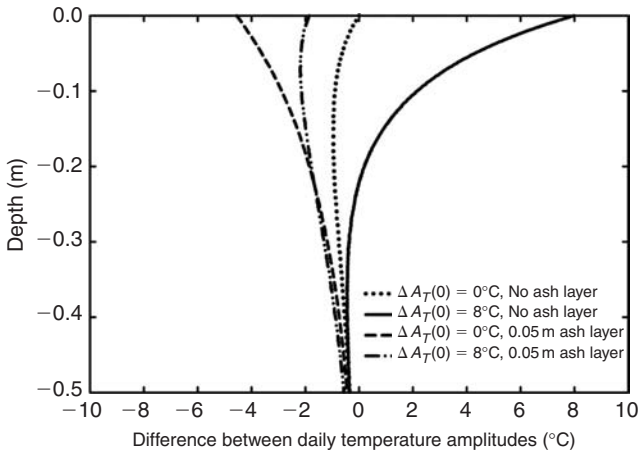

Fig. 8. Model profiles of temperature amplitude differences (burn minus no-burn) during the daily heating cycle of a moist soil (see Table 1) for different upper boundary conditions at the soil surface, $A_T(ss)$. From left to right these are: (1) $A_T(ss) = (12°C) \times \exp(-z_{ash}/D_{ash})$ for the burn area and $A_T(ss) = 12°C$ for the no-burn area; (2) $A_T(ss) = (26°C) \times \exp(-z_{ash}/D_{ash})$ for the burn area and $A_T(ss) = 18°C$ for the no-burn area; (3) $A_T(ss) = 12°C$ for the burn area and $A_T(ss) = 12°C$ for the no-burn area; (4) $A_T(ss) = 26°C$ for the burn area and $A_T(ss) = 18°C$ for the no-burn area. For the two ash-covered soils, the ash layer depth, z_{ash}, is assumed to be 0.05 m and D_{ash} is 0.105 m for a moist soil and 0.060 m for a dry soil.

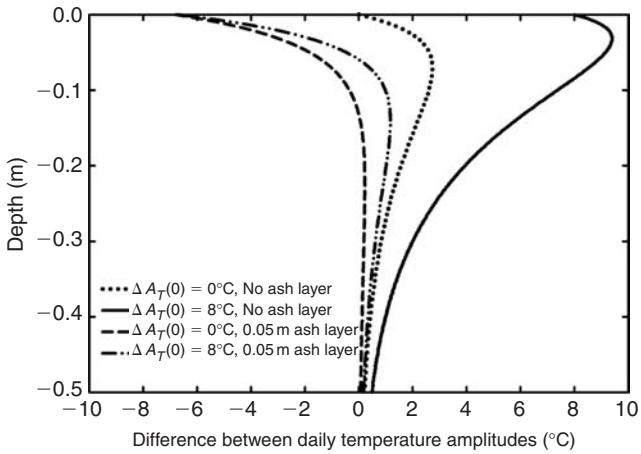

Fig. 9. Model profiles of temperature amplitude differences (burn minus no-burn) during the daily heating cycle of a dry soil (see Table 1) for different upper boundary conditions at the soil surface, $A_T(ss)$. From left to right these are: (1) $A_T(ss) = (12°C) \times \exp(-z_{ash}/D_{ash})$ for the burn area and $A_T(ss) = 12°C$ for the no-burn area; (2) $A_T(ss) = (26°C) \times \exp(-z_{ash}/D_{ash})$ for the burn area and $A_T(ss) = 18°C$ for the no-burn area; (3) $A_T(ss) = 12°C$ for the burn area and $A_T(ss) = 12°C$ for the no-burn area; (4) $A_T(ss) = 26°C$ for the burn area and $A_T(ss) = 18°C$ for the no-burn area. For the two ash-covered soils, the ash layer depth, z_{ash}, is assumed to be 0.05 m and D_{ash} is 2.01 m for a moist soil and 1.15 m for a dry soil.

Fig. 8 shows four simulated profiles of the difference in the temperature amplitudes associated with the daily soil heating cycle for a moist soil. In general, for a moist soil the amplitude of the daily temperature cycle, $A_T(z)$, is greater at the no-burn site than at the burn site, this is true for all simulations below about 0.20 m. The exception to this (the rightmost curve) occurs in the upper few centimeters of soil whenever $A_T(z)$ is much greater for the burn area than the no-burn area. These results suggest that the main affect that a burn will have on the daily heating cycle of a wet soil is to reduce the daily extremes that will occur in the soil, except for the upper portion of the soil, where the changes in surface properties cause the surface forcing, $A_T(0)$, to increase within a burn area relative to the no-burn area.

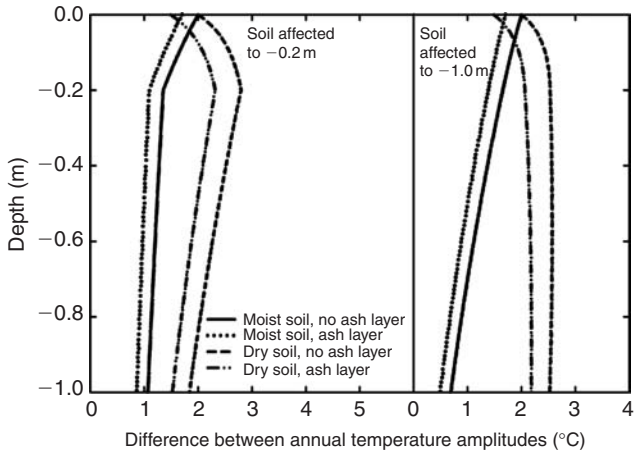

Fig. 10. Model profiles of temperature amplitude differences (burn minus no-burn) associated with the annual heating cycle for both a moist and a dry soil (see Table 1) for different upper boundary conditions at the soil surface, $A_T(ss)$. The left panel, which consists of four curves, assumes that the fire-affected soil thermal properties extend only through the upper 0.2 m of soil, whereas the four curves in the right panel assume that the he fire-affected soil thermal properties extend to 1.0 m deep. For each panel the two parallel curves that decrease with depth (leftmost) are for a moist soil. $A_T(ss)$ for these two curves are from left to right: (1) $A_T(ss) = (12°\text{C}) \times \exp(-z_{ash}/D_{ash})$ for the burn area and $A_T(ss) = 10°\text{C}$ for the no-burn area; (2) $A_T(ss) = 12°\text{C}$ for the burn area and $A_T(ss) = 10°\text{C}$ for the no-burn area. The other two parallel curves (rightmost) within each panel are for a dry soil. $A_T(ss)$ for these two curves are from left to right: (3) $A_T(ss) = (12°\text{C}) \times \exp(-z_{ash}/D_{ash})$ for the burn area and $A_T(ss) = 10°\text{C}$ for the no-burn area; (4) $A_T(ss) = 12°\text{C}$ for the burn area and $A_T(ss) = 10°\text{C}$ for the no-burn area. For the ash-covered soils, the ash layer depth, z_{ash}, is assumed to be 0.05 m and D_{ash} for a moist and dry soil is the same as Figs 8 and 9.

Fig. 9 shows the four simulated profiles of difference in the temperature amplitudes associated with the daily soil heating cycle for a dry soil. In the no-ash case (two rightmost curves), which probably reflect the most common situation at the first two MEF burn sites, the maximum difference in $A_T(z)$ does not occur at the surface. It occurs between 0.02 and 0.06 m beneath the soil surface and the increase of the daily temperature amplitude within this region is between 3 and 9°C. In the case of the profile with the 3°C increase there is no difference in the surface forcing, i.e., $A_T(0) = 12°\text{C}$ for both the burn and no-burn simulations. So this maximum of the soil temperature difference below the soil surface occurs solely as a result of the change in soil thermal properties caused by the burn. Either of the no-ash simulations suggest a significant change in the normal thermal environment of the soil as a result of the fire. Even in the case of an ash layer (two leftmost curves) the amplitude difference still tends to be positive below about 0.15-m depth, despite a significant reduction in A_T at the soil surface within the burn area. Therefore, for a dry MEF soil, the burns have caused the amplitude of the daily extremes to increase relative to a no-burn area.

Fig. 10 is comprised of two panels of four simulations each. The only difference between these two panels is that the simulations on the left restrict the fire-affected thermal properties to only the top 0.2 m of soil, whereas the right panel extends throughout the entire soil profile. Comparing the corresponding simulations between panels indicates the model's sensitivity to the continuity assumption concerning the soil thermal properties discussed above. Taken together, these panels can be interpreted as bounding or endpoint conditions on the difference profiles that are likely to occur naturally. Each panel shows four simulated profiles of the difference in the temperature amplitudes associated with the annual soil heating cycle for a wet soil with and without as ash layer (two leftmost curves) and a dry soil with and without an ash layer (two rightmost curves). In general the ash layer has much less impact on the annual temperature profile than the daily profile, which should not be too surprising given the previous discussion concerning attenuation depth of ash. But, unlike the daily cycle, the amplitude of the extremes in temperature is greater for both wet and dry burn area soil than

Table 1. Model parameters for fire-affected and unaffected soils for two different soil moisture characterisations. The last two columns on the right are for the daily cycle of soil heating and cooling. The difference in $\overline{T}(0)$ between the burn and no-burn areas were taken from the maximum temperatures of the annual cycle, shown in Fig. 7. The ratio $A_G(0)/A_T(0)$ is a bulk measure of the influence that the thermal properties and their vertical structure have on the daily cycle of heat propagation through the soil

Moisture status	θ_0 [$m^3\,m^{-3}$]	α_θ [m^{-1}]	C_0 [$MJ\,m^{-3}\,K^{-1}$]	α_c [m^{-1}]	λ_0 [$W\,m^{-1}\,K^{-1}$]	α_λ [m^{-1}]	$\overline{T}(0)$ [°C]	$A_G(0)/A_T(0)$ [$W\,m^{-2}\,°C^{-1}$]
				No-burn soil				
Dry	0.0	0.15	0.91	1.67	0.15	9.33	20	3.63
Moist	0.2	0.49	1.75	1.68	1.79	2.33	20	17.06
				Burn soil				
Dry	0.0	0.15	0.92	1.67	0.58	1.68	22	6.90
Moist	0.2	0.49	1.75	1.68	1.12	1.69	22	13.24

the corresponding no-burn area soil. This is true regardless of the continuity assumption. The primary reason for this is that the amplitude of the surface forcing at the burn area is 2°C greater than the no-burn area (22°C *v.* 20°C, see Fig. 7). For a wet MEF soil these extremes diminish with depth, but they are still significant even at 1.0-m depth. For a dry soil the amplitude of these extremes increases with depth until somewhere between 0.2 and 0.9 m in depth before they begin to diminish. As with the daily cycle, the maximum temperature effects caused by fire are not necessarily at the surface, but occur deeper in the soil profile. Even at 1.0-m depth, the annual temperature maximum for a dry soil could be as much as 1.9 (left panel) to 2.5°C (right panel) greater within the burn area soil than the no-burn soil. Again this corresponds to a significant change in the long-term soil thermal regime as a consequence of the fire. [Note: although not explicitly included in Figs 8 and 9, the model's sensitivity to the continuity assumption is less for the daily cycle than that shown in Fig. 10 for the annual cycle.]

Figs 8, 9, and 10 are based on Eqn 16, the approximate solution to the soil heat flow equation. An important expectation for this approximate solution is that $\alpha_c < \alpha_\lambda$. Although the parameter values listed in Table 1 confirm that $\alpha_c < \alpha_\lambda$ and that $\alpha_c z_m < 1$ as well, the fire-induced changes in α_λ are so great that it is also possible to argue that $\alpha_\lambda \approx \alpha_c$ might provide a better solution for the temperature profiles shown in Figs 8, 9, and 10. We tested this possibility by using $\alpha_\lambda = \alpha_c$ and Eqn 15 in place of Eqn 16. The only difference between the two models was that the present approximate model underestimated the heat flux relative to the $\alpha_\lambda = \alpha_c$ model by less that 5% near the surface. Otherwise the resulting profiles for temperature and heat flux were nearly identical with those shown in Figs 8, 9, and 10, further confirming that Eqn 16 is a reasonable model for $A_T(z)$.

Table 1 also includes the model-derived parameter $A_G(0)/A_T(0)$, which can be thought of as a generalization of the soil's thermal admittance [$\mu_s \equiv \sqrt{C_s \lambda_s}$], but specified at the soil surface. In the case of a soil with uniform thermal properties $A_G(0)/A_T(0) = \sqrt{\omega}\mu_s$ (e.g. van Wijk and DeVries 1963). But in the present case the soils are non-uniform, so the ratio $A_G(0)/A_T(0)$ includes additional factors related to the vertical profiles of the thermal properties [e.g. Eqns 16 and 18]. Although Table 1 includes those values of $A_G(0)/A_T(0)$ that are appropriate to daily forcing, the same general pattern and any associated interpretations apply to the annual forcing as well. The thermal admittance has been used with studies of the effects that the near-soil-surface microclimate can have on seedling survival (e.g. Hungerford and Babbitt 1987) and how surface energy partitioning is affected by the vertical structure of the soil thermal properties (e.g. Novak 1986). The ratio $A_G(0)/A_T(0)$ shares these qualities. The utility of $A_G(0)/A_T(0)$ to the present study is that it provides a single bulk measure of the consequences of the changes in the soil thermal properties caused by the soil heating during the fire. The most significant long-term change to $A_G(0)/A_T(0)$ occurs when the soil is dry, for which $A_G(0)/A_T(0)$ at the burn area is almost twice that of the no-burn area. Thus MEF burn area soils when dry will be much more efficient at conducting or propagating thermal energy than the no-burn area soils. Just the opposite is true in the case of moist soil. Nevertheless, a moist soil will always be much more thermally efficient than a dry soil. These changes in the $A_G(0)/A_T(0)$ suggest that the effects of the fire on the soil will be much greater when the soil is dry than when it is moist, in agreement with implications of Fig. 5 and the results shown in Figs 8, 9, and 10.

Before closing we should point out that the model results have largely been focused on periods when the soil temperatures are above freezing. This is by intention. But, in order to maintain this focus, we have implicitly assumed that near 0°C the thermal properties of liquid water and ice are about the same. This is clearly not the case. Near 0°C the specific heat of ice is about half that of water and the thermal conductivity of ice is about four times as much as water's (List 1971). It is beyond the intent and scope of the present study to develop a model of the thermal energy flow in a soil that includes a realistic freeze-thaw cycle. Nonetheless, given the surprising nature of the present results and their implications to the functioning and recovery of soil's biota throughout the soil profile, a study of the frozen soil's thermal properties and thermal regime seems warranted.

Conclusions

Soils beneath two experimental slash piles within the Manitou Experimental Forest were affected by the extreme heating that occured when the piles were burned. The soil thermal conductivity, and in particular the relationship between it and the soil bulk density and soil moisture, changed dramatically as a consequence of these prescribed burns. But, the soil bulk density itself was not changed by the intense soil heating. Nevertheless, the fire-induced effects result (we hypothesise) from long-term structural changes inherent to the soil because they are not due simply to loss of soil moisture during the burns or to changes in soil bulk density. We describe these changes as long-term because at one burn site they were clearly detectable 3.75 years after the soil had cooled. Unfortunately, the nature of this inferred structural change cannot be determined from any observations or data obtained during this experiment.

Results of this study also clearly indicate that prescribed burns can have a long term effect on the soil surface temperatures. At one burn site the amplitude of the daily cycle of soil heating and cooling could be as much as 10°C greater within the burn area than at a nearby no-burn area. Whereas for the annual cycle, the amplitude difference was about 2°C greater.

Combining the observed long-term changes in the soil thermal conductivity, the observed changes to its vertical structure, and the changes in the amplitudes associated with the daily and annual cycles of soil surface heating with a model of heat propagation in soils, this study also explores the long-term consequences that the extreme soil heating during prescribed burns can have to the thermal climate of the burn area soil. In addition this model also includes a simple formulation of an ash layer so that possible long-term soil effects resulting from a residual ash layer are considered as well. The thermal properties of ash used with this model were obtained from an experimental burn and are some of the first observations of their kind ever made.

The modeling results indicate when the soil at the experimental forest is dry and does not include a significant ash layer the daily and annual extremes of temperature and heat flux are likely to be significantly greater for the burn area than for no-burn area. On the other hand, when the same soil is moist, the temperature

extremes are reduced. But because of the changes in the vertical structure of the soil thermal conductivity, the model results also indicate that these maximum differences do not necessarily occur at the soil surface. Rather for dry soils in particular they can occur between 0.02 and 0.06 m deep during the daily heating and cooling cycle and between 0.2 and 0.9 m deep during the annual cycle. Below these depths the long-term temperature effects do diminish; nonetheless, they can remain significant to much greater depths. As should be expected, the modeling results suggest that the presence of an ash layer does insulate the soil, thereby reducing the temperature extremes that would otherwise occur in the soil, and that the effect depends on the ash layer depth and the frequency of the periodic forcing. Nevertheless, these long-term effects of ash layers on soils are intended to be qualitative. Factors that determine the long-term persistence of an ash layer, such as its stability and erodibility, are not part of this study.

Acknowledgements

We wish to thank Dr. M. A. Karam for his assistance in implementing his thermal wave model of heat propagation in nonuniform soils so that we could check the quality of our approximate analytical solution for the profiles of soil temperature and heat flux. We also wish to thank Dr. G. J. Kluitenberg for his comments on the final version of this manuscript.

References

Andrews LC (1992) 'Special functions of mathematics for engineers.' 2nd edn. pp. 311–312. (McGraw-Hill: New York, NY)

Badía D, Martí C (2003) Plant ash and heat intensity effects on chemical and physical properties of two contrasting soils. *Arid Land Research and Management* **17**, 23–41. doi:10.1080/15324980301595

Beringer J, Hutley LB, Tapper NJ, Coutts A, Kerley A, O'Grady AP (2003) Fire impacts on surface heat, moisture and carbon fluxes from a tropical savanna in northern Australia. *International Journal of Wildland Fire* **12**, 333–340. doi:10.1071/WF03023

Bristow KL (2002) Thermal Conductivity. In 'Methods of soil analysis'. (Co-Eds JH Dane, GC Clarke) pp. 1209–1226. (Soil Science Society of America: Madison, WI)

Campbell GS, Jungbauer JD Jr, Bidlake WR, Hungerford RD (1994) Predicting the effect of temperature on soil thermal conductivity. *Soil Science* **158**, 307–313.

Campbell GS, Norman JM (1998) 'An introduction to environmental biophysics.' 2nd edn. (Springer-Verlag: New York, NY)

DeBano LF, Neary DG, Ffolliott PF (1999) 'Fire's effects on ecosystems.' (John Wiley & Sons: New York, NY)

DeBano LF, Neary DG, Ffolliott PF (2005) Chapter 2: Soil physical properties. In 'Wildland fire in ecosystems: effects of fire on soil and water'. USDA Forest Service, Rocky Mountain Research Station General Technical Report RMRS-GTR-42-vol.4. (Eds DG Neary, KC Ryan, LF DeBano) pp. 29–51. (Ogden, UT)

DeVries DA (1963) Thermal properties of soils. In 'Physics of plant environment'. (Ed. WR van Wijk) pp. 210–235. (John Wiley & Sons: New York, NY)

Farouki OT (1986) 'Thermal properties of soils.' (Trans Tech Publications: Clausthal-Zellerfeld, Germany)

Hopmans JW, Dane JH (1986) Thermal conductivity of two porous media as a function of water content, temperature, and density. *Soil Science* **142**, 187–195. doi:10.1097/00010694-198610000-00001

Huffman EL, MacDonald LH, Stednick JD (2001) Strength and persistence of fire-induced soil hydrophobicity under ponderosa and lodgepole pine, Colorado Front Range. *Hydrological Processes* **15**, 2877–2892. doi:10.1002/HYP.379

Hungerford RD, Babbitt RE (1987) 'Overstory removal and residue treatments affect soil surface, air and, soil temperature: Implications for seedling survival.' USDA Forest Service, Intermountain Research Station Research Paper INT-377. (Ogden, UT)

Iverson LR, Hutchinson TF (2002) Soil temperature and moisture fluctuations during and after prescribed fire in mixed-oak forests, USA. *Natural Areas Journal* **22**, 296–304.

Jury WA, Gardner WR, Gardner WH (1991) 'Soil physics.' 5th edn. (John Wiley: Hoboken, NJ)

Karam MA (2000) A thermal wave approach for heat transfer in a nonuniform soil. *Soil Science Society of America Journal* **64**, 1219–1225.

Kay BD, Goit JB (1975) Temperature-dependent specific heats of dry soil materials. *Canadian Geotechnical Journal* **12**, 209–212.

Knoepp JD, DeBano LF, Neary DG (2005) Chapter 3: Soil chemistry. In 'Wildland fire in ecosystems: effects of fire on soil and water'. (Eds DG Neary, KC Ryan, LF DeBano) pp. 53–71. USDA Forest Service, Rocky Mountain Research Station General Technical Report RMRS-GTR-42-vol.4. (Ogden, UT)

List RJ (1971) 'Smithsonian meteorological tables.' 6th revised edn; 5th reprint. (Smithsonian Institution Press: Washington, DC)

Massman WJ (1993) Periodic temperature variations in an inhomogeneous soil: a comparison of approximate and analytical expressions. *Soil Science* **155**, 331–338. doi:10.1097/00010694-199305000-00004

Massman WJ, Frank JM (2004) The effect of a controlled burn on the thermophysical properties of a dry soil using a new model of soil heat flow and a new high temperature heat flux sensor. *International Journal of Wildland Fire* **13**, 427–442. doi:10.1071/WF04018

Massman WJ, Frank JM, Jiménez Esquilin AE, Stromberger ME, Shepperd WD (2006) Long term consequences of a controlled slash burn and slash mastication to soil moisture and CO_2 at a southern Colorado site. In '27th Conference on Agricultural and Forest Meteorology'. (American Meteorological Society: Boston, MA) [Available on CD from the AMS and at http://ams.confex.com/ams/BLTAgFBioA/techprogram/programexpanded_352.htm]

Massman WJ, Frank JM, Shepperd WD, Platten MJ (2003) In situ soil temperature and heat flux measurements during controlled surface burns at a southern Colorado forest site. In 'Fire, fuel treatments, and ecological restoration: Conference proceedings, 16–18 April 2002, Fort Collins, CO'. USDA Forest Service, Rocky Mountain Research Station Proceedings RMRS-P-29. (Eds PN Omi, LA Joyce) pp. 69–87. (Fort Collins, CO)

Neary DG, Ffolliott PF (2005) 'Part B – The Water Resource: It's importance, characteristics, and general responses to fire.' USDA Forest Service, Rocky Mountain Research Station General Technical Report RMRS-GTR-42-vol.4. (Eds DG Neary, KC Ryan, LF DeBano) pp. 95–106. (Ogden, UT)

Neary DG, Ryan KC, DeBano LF, Landsberg JD, Brown JK (2005) 'Chapter 1: Introduction.' USDA Forest Service, Rocky Mountain Research Station General Technical Report RMRS-GTR-42-vol.4. (Eds DG Neary, KC Ryan, LF DeBano) pp. 1–17. (Ogden, UT)

Nerpin SV, Chudnovskii AF (1984) 'Heat and mass transfer in the plant-soil-air system.' pp. 33–50. (Oxonian Press Pvt. Ltd.: New Delhi)

Novak MD (1986) Theoretical values of daily atmospheric and soil thermal admittances. *Boundary-Layer Meteorology* **34**, 17–34. doi:10.1007/BF00120906

Page-Dumroese DP, Jurgensen MF, Tairks AE, Ponder F Jr, Sanchez FG, *et al.* (2006) Soil physical property changes at the North America long-term soil productivity study sites: 1 and 5 years after compaction. *Canadian Journal of Forest Research* **36**, 551–564. doi:10.1139/X05-273

Retzer JL (1949) 'Soils and physical conditions at Manitou Experimental Forest.' Rocky Mountain Forest and Range Experiment Station. (Fort Collins, CO)

Seymour G, Tecle A (2004) Impact of slash pile size and burning on ponderosa pine forest soil physical properties. *Journal of the*

Arizona-Nevada Academy of Science **37**, 74–82. doi:10.2181/1533-6085(2004)037<0074:IOSPSA>2.0.CO;2

Spanier J, Oldham KB (1987) 'An atlas of functions.' (Hemisphere Publishing Corp.: Washington, DC)

Tan X, Chang SX, Kabzems R (2005) Effects of soil compaction and forest floor removal on soil microbial properties and N transformations in a boreal forest long-term soil 38 productivity study. *Forest Ecology and Management* **217**, 158–170. doi:10.1016/J.FORECO.2005.05.061

US Department of Agriculture (1986) 'Soil Survey of Pike National Forest, Eastern Part, Colorado, Parts of Douglas, El Paso, Jefferson, and Teller Counties.' USDA Forest Service, Soil Conservation Service, Colorado Agricultural Experiment Station. (Fort Collins, CO)

van Wijk WR, Derksen WJ (1963) Sinusoidal temperature variation in a layered soil. In 'Physics of plant environment'. (Ed. WR van Wijk) pp. 171–209. (John Wiley & Sons: New York, NY)

van Wijk WR, DeVries VA (1963) Periodic temperature variations in a homogeneous soil. In 'Physics of plant environment'. (Ed. WR van Wijk) pp. 102–143. (John Wiley & Sons: New York, NY)

Wagner W, Pruss A (2002) The IAPWS formulation 1995 for the thermophysical properties of ordinary water substance for general and scientific use. *Journal of Physical and Chemical Reference Data* **31**, 387–535. doi:10.1063/1.1461829

Whitehead CS (1911) On a generalization of the functions ber x, bei x, ker x, kei x. *Quarterly Journal of Pure Applied Mathematics* **42**, 316–342.

Whyte AC (1998) Kelvin Functions and their derivatives. Available at http://www.acwhyte.fsnet.co.uk/kelgenpaper.htm [Verified 29 January 2008]

Wierenga PJ, Nielsen DR, Hagan RM (1969) Thermal properties of a soil based upon field and laboratory measurements. *Soil Science Society of America Proceedings* **33**, 354–360.

Manuscript received 25 August 2006, accepted 13 August 2007

Appendix. The influence of temperature on the thermal properties of soil

Temperature directly affects both the volumetric specific heat and the thermal conductivity of soil. When modeling the extreme soil heating that occurs during a fire, these effects must be included because they can become very large. In turn this means that the thermal properties of the medium (the soil) are themselves changing in response to or are coupled to the thermal pulse as it moves through the soil, thereby introducing some important nonlinearities into the heat flow equation. The same thing occurs during the daily and annual heating of the soil, but the heat pulse is much less than that which occurs during a fire so the nonlinearities are also significantly reduced. This appendix examines these nonlinear effects for the daily and annual cycles of soil heating and cooling.

Measurements of the specific heat capacity of Manitou Experimental Forest (MEF) soil at different temperatures, c_s, suggests that $c_s = c_s(T) = 0.72 + \Delta_{cT} T$, where $\Delta_c = 0.002\,\mathrm{J\,g^{-1}\,K^{-1}\,{}^{\circ}C^{-1}}$ and T is the temperature [°C]. Using Eqns 14 and 16 $T = \overline{T}(z) + A_T(z) \approx \overline{T}(0) + \alpha_T z + A_T(z)$, where $-[\overline{G}(0)/(\alpha_\lambda \lambda_0)]\ln(1+\alpha_\lambda z) \approx \alpha_T z$, and $\alpha_T = -\overline{G}(0)/\lambda_0$.

Therefore, $c_s(T) \approx 0.72 + \Delta_{cT}\overline{T}(0) + \Delta_{cT}\alpha_T z + \Delta_{cT} A_T(z)$. Observations suggest that α_T will vary with time of year, but that in general $|\alpha_T| < 50\,\mathrm{m^{-1}}$. Because this study focuses primarily on the upper 0.2 m of soil, it follows that $\Delta_{cT}|\alpha_T|z < 0.02\,\mathrm{J\,g^{-1}\,K^{-1}}$ for $0 \le z \le z_m = 0.2$ m. Given that the maximum value of $\overline{T}(0)$, which will occur at about the same time as the maximum of $|\alpha_T|$, can exceed 40°C, it follows that the term $\Delta_{cT}|\alpha_T|z < \Delta_{cT}\overline{T}(0)$ throughout the soil profile and throughout annual cycle. Similarly from observations $A_T(z)$ at 0.20-m depth can be about 10°C at the same time that $|\alpha_T|$ is a maximum, so that at about 0.2-m depth the term $\Delta_{cT}A_T(z)$ should further reduce or cancel the effects of the term $\Delta_{cT}\alpha_T z$ can have on c_s. To first order then the effects of the $\Delta_{cT}\alpha_T z$ term can be ignored. The other non-linear term $\Delta_{cT}A_T(z)$ tends to be greater than $\Delta_{cT}\alpha_T z$. In fact $\Delta_{cT}A_T(z)$ can approach 10% of the term $c_{s0} = 0.72 + \Delta_{cT}\overline{T}(0)$ near the surface. For the present study, this was deemed small enough to ignore. A similar mathematical argument can be developed for the effects that $A_T(z)$ can have on C_w (see main text). But these effects contribute less that 3% to C_w used in this study, so they can be safely ignored.

Documenting the temperature effects on the thermal conductivity of soil, λ_s, is important because the λ_s data were obtained in situ, which means they implicitly include the effects of the soil temperature at the time and the depth of the measurements. Therefore, it is valuable to know any possible significance these effects may have to the data.

Over the temperature range 23–100°C the thermal conductivity data for dry MEF soil, which were analysed by Thermophysical Properties Research Laboratory, showed that $\lambda_s(T) = \lambda_{sd} + \Delta_{\lambda d} T$. Within the slash pile burn area before the experimental burn $\lambda_{sd} = 0.19 \pm 0.02\,\mathrm{W\,m^{-1}\,K^{-1}}$ and $\Delta_{\lambda d} = 2.9 \pm 0.3 \times 10^{-4}\,\mathrm{W\,m^{-1}\,K^{-1}\,{}^{\circ}C^{-1}}$; whereas after the burn $\lambda_{sd} \approx 0.54 \pm 0.20\,\mathrm{W\,m^{-1}\,K^{-1}}$ and $\Delta_{\lambda d} \approx 3.5 \pm 8.0 \times 10^{-4}\,\mathrm{W\,m^{-1}\,K^{-1}\,{}^{\circ}C^{-1}}$. The change in λ_{sd} is consistent (but not the same as) the change in A between the burn and no-burn areas (see main text). That is λ_{sd} increased by a factor of 2.8 [= 0.54/0.19] as a result of the fire, whereas A increased by a factor of about 4 [= 0.486/0.123]; this was mentioned in the text. On the other hand, the slope, $\Delta_{\lambda d}$, does not appear to have changed very much as a result of the burn. But we cannot claim that $\Delta_{\lambda d}$ has not changed, even though the pre- and post-burn values of $\Delta_{\lambda d}$ are similar. The post-fire value of $\Delta_{\lambda d}$ is skewed by one of the four samples. Disregarding that one sample yields $\Delta_{\lambda d} \approx 0.78 \pm 1.0 \times 10^{-4}\,\mathrm{W\,m^{-1}\,K^{-1}\,{}^{\circ}C^{-1}}$, which is significantly lower that the pre-burn value. In fact, it probably could be argued that the post-burn value of $\Delta_{\lambda d}$ is not statistically different from $0.0\,\mathrm{W\,m^{-1}\,K^{-1}\,{}^{\circ}C^{-1}}$. For the present purposes we assume that the post-burn value of $\Delta_{\lambda d}$ equals the pre-burn value of $2.9 \pm 0.3 \times 10^{-4}\,\mathrm{W\,m^{-1}\,K^{-1}\,{}^{\circ}C^{-1}}$.

The above pre- and post-burn values of λ_{sd} and $\Delta_{\lambda d}$, along with observations of $\overline{T}(0) + A_T(0)$, can now be used to estimate the maximal temperature effects on a dry soil value of λ_s. From the burn and no-burn observations $\overline{T}(0) + A_T(0) \le 60$°C, therfore, $\Delta_{\lambda d}[\overline{T}(0) + A_T(0)]/\lambda_{sd} < 10\%$ for a pre- or no-burn dry soil. The significance of temperature effects on the burn soil is less that 4%, which is even smaller.

To determine the effects of temperature on λ_s when the soil is moist requires using the moist soil analogues to λ_{sd} and $\Delta_{\lambda d}$. These values are the values that are appropriate to water (denoted, λ_w and $\Delta_{\lambda w}$) weighted by the amount of soil moisture within the soil. For water $\lambda_w = 0.56\,\mathrm{W\,m^{-1}\,K^{-1}}$ and $\Delta_{\lambda w} = 1.8 \times 10^{-3}\,\mathrm{W\,m^{-1}\,K^{-1}\,{}^{\circ}C^{-1}}$. Fig. 5 shows that for all the data used in this study $\theta_v < 0.23$ and that most of the time $\theta_v < 0.10$. Therefore the maximal temperature effects on λ_s when the soil is moist will be somewhat greater than for a dry soil, but are not likely to exceed an additional 10%.

In summary, the most significant effects temperature can have on the values soil thermal properties at MEF during the daily and annual cycles of soil heating are likely to be about 10% (or possibility as much as 20% in the case of thermal conductivity of a very moist soil) and that they will be of greatest consequence near the soil surface and that they will diminish as the soil temperature deceases with depth.